



# Identification and Validation of 17-lncRNA Related to Regulatory T Cell Heterogeneity as a Prognostic Signature for Head and Neck Squamous Cell Carcinoma

Qi Sun<sup>1,2†</sup>, Yumei Li<sup>1,2†</sup>, Xin Yang<sup>1,2†</sup>, Xinxin Wu<sup>1,2</sup>, Zhen Liu<sup>1,2</sup>, Yakui Mou<sup>1,2\*</sup> and Xicheng Song<sup>1,2\*</sup>

<sup>1</sup> Department of Otorhinolaryngology, Head and Neck Surgery, Yantai Yuhuangding Hospital, Qingdao University, Yantai, China, <sup>2</sup> Shandong Provincial Clinical Research Center for Otorhinolaryngologic Diseases, Yantai Yuhuangding Hospital, Yantai, China

## OPEN ACCESS

### Edited by:

Silvia Deaglio,  
University of Turin, Italy

### Reviewed by:

Dapeng Lei,  
Shandong University, China  
Wen G. Jiang,  
Cardiff University, United Kingdom

### \*Correspondence:

Xicheng Song  
dxchsong@163.com  
Yakui Mou  
muykmd@126.com

<sup>†</sup>These authors have contributed  
equally to this work

### Specialty section:

This article was submitted to  
T Cell Biology,  
a section of the journal  
Frontiers in Immunology

**Received:** 24 September 2021

**Accepted:** 03 November 2021

**Published:** 22 November 2021

### Citation:

Sun Q, Li Y, Yang X, Wu X, Liu Z, Mou Y and Song X (2021) Identification and Validation of 17-lncRNA Related to Regulatory T Cell Heterogeneity as a Prognostic Signature for Head and Neck Squamous Cell Carcinoma. *Front. Immunol.* 12:782216. doi: 10.3389/fimmu.2021.782216

Successful eradication of tumors by the immune system depends on generation of antigen-specific T cells that migrate to tumor sites and kill cancerous cells. However, presence of suppressive Treg populations inside tumor microenvironment hinders effector T cell function and decreases antitumor immunity. In this study we independently evaluated and confirmed prognostic signature of 17-Treg-related-lncRNA. Immune cell infiltration analysis using 17-lncRNA signature as a probe, accurately described Treg populations in tumor immune microenvironment. 17-lncRNA signature model predicted prognosis with excellent accuracy in all three cohorts: training cohort (AUC=0.82), testing cohort (AUC=0.61) and total cohort (AUC=0.72). The Kaplan-Meier analysis confirmed that the overall survival of patients in the low-risk group was significantly better than those in the high-risk group (P<0.001). CIBERSORT analysis confirmed that low risk group had higher infiltration of tumor killer CD8 T cells, memory activated CD4 T cells, follicular helper T cells and T cells regulatory (Tregs), and lower expression of M0 macrophages and Mast cells activated. These results indicate that the 17-lncRNA signature is a novel prognostic and support the use of lncRNA as a stratification tool to help guide the course of treatment and clinical decision making in patients at high risk of HNSCC.

**Keywords:** regulatory T cell heterogeneity, long non-coding RNA, prognostic signature, immune cell infiltration, head and neck squamous cell carcinoma

## INTRODUCTION

Squamous cell carcinoma of the head and neck is the sixth most common cancer in the world (1). A 5-year survival rate for patients with HNSCC is lower than 50%–55%, mainly due to local recurrence or metastasis (2, 3). The immunotherapy response rate of recurrent or metastatic HNSCC is largely driven by tumor immune microenvironment (TME) and is notoriously poor. A

better understanding of TME in HNSCC is critical for the immune therapy to infuse new hope into HNSCC patients. To that end, identification of TME specific biomarkers that can effectively predict efficacy of immune therapy is crucial for proper patient selection.

Tumor infiltrating Tregs which are part of tumor microenvironment are thought to hinder local anti-tumor immune response by mediating tumor immune escape and accelerating its progression (4–6). However, conflicting data regarding poor prognostic value of Tregs raised a possibility of two distinct subtypes present in different tumor types: (I) suppressive Tregs, which are CD4 T cells that express CD45 receptor in both resting and activated states and (II) nonsuppressive Tregs, which are CD45 receptor negative CD4 T cells (7). Infiltration of TME with immunosuppressive Tregs inhibits T cell effector function (8, 9) and NK cell-mediated cytotoxicity (10) leading to poor prognosis and high recurrence of most cancers, including breast and lung cancer. By the same token, presence of non-immunosuppressive Tregs in colorectal cancer (CRC), known to secrete pro-inflammatory cytokines (11), leads to a better prognosis than those infiltrated with suppressive Tregs (12). Mechanistically, nonsuppressive Tregs may benefit the host by inhibiting low levels bacteria-driven inflammation (13).

There are previous reports that have noted that expression of lncRNA correlates with specific Treg subtype expressed during carcinogenesis (14, 15). For example, LINC00301 lncRNA is highly expressed in non-small cell lung cancer. Its expression targets TGF- $\beta$  which leads to an increase in a number of immunosuppressive Tregs and a decrease of the CD8T cell positive population in LA-4/SLN-205-derived tumors (15). In hepatocellular carcinoma (HCC), lnc-EGFR (epidermal growth factor receptor) was shown to promote differentiation of immunosuppressive Tregs offering a new therapeutic target for HCC (14, 15). However, which lncRNA specifically regulate Treg cell heterogeneity in HNSCC patients remains unknown.

In this study, we identified a unique 17-lncRNA signature using Univariate Cox and LASSO analysis followed by multivariate Cox regression signature construction. Kaplan-Meier analysis, ROC analyses, and multivariate Cox regression confirmed that THRL signature is indeed a novel, unique and important prognostic factor. 17-lncRNA signature correlated with the infiltration status of Treg cells, and is a true measure of tumor immune microenvironment in HNSCC. Our study will allow for better clinical decision making in evaluating HNSCC patients who will benefit from immunotherapy.

## METHODS

### Data Sets and Sample Extraction

RNA sequencing data sets together with the corresponding clinical characteristics of patients with HNSCC were downloaded from The Cancer Genome Atlas (TCGA, <https://cancergenome.nih.gov/>). Manual reannotation of RNA-seq data sets was used to separate expression data into mRNA and

lncRNA. The expression levels were transformed as  $\log_2(x+1)$  and standardized (16). Originally, RNA-seq data sets from 546 patients with HNSCC was collected. Only, 453 cases with complete follow-up data which included survival time  $\geq 30$  days, clinicopathological profile were included in the follow-up analysis.

### Acquisition of Treg-Related mRNA

The GSE15659 dataset, downloaded from the Gene Expression Omnibus (GEO, <https://www.ncbi.nlm.nih.gov/geo/>) DataSets, contains five T cell subtypes, including 2 suppressive Treg cell subpopulations, and nonsuppressive Treg cell subpopulations, named as Group 1 and Group 2 in our study, respectively. The dataset was based on the GPL570 platform (Affymetrix Human Genome U133 Plus 2.0 Array). Specifically, we reannotated the probe set by the affymetrixHgU133Plus2.0 array and ensured that the probes mapped to the genome were unique. We analyzed the expression differences of transcripts including mRNA and lncRNA between groups 1 and 2 according to the standard of  $|\log_2FC| > 1$  and P value  $< 0.05$ . The differential mRNAs in GSE15659 were crossed with mRNAs obtained from the expression profiles of patients with HNSCC from the TCGA database, and the crossed mRNAs were listed as Treg-related mRNAs.

### Identification of Treg-Related lncRNA

All patients with HNSCC were randomly divided into training and testing cohorts according to their survival status at the ratio of 1:1 (16). In the training cohort, the correlation score between lncRNAs obtained from TCGA data set and Treg-related mRNAs were calculated by Person correlation coefficient test. lncRNAs that correlated with Treg-related mRNAs were selected for subsequent analysis according to the following criteria of  $|\text{correlation coefficient}| > 0.6$  and  $P < 0.001$  (17–19). Finally, a Treg-related mRNAs-lncRNAs co-expression network was constructed according to the criteria of  $|\text{correlation coefficient}| > 0.3$  and  $P < 0.001$  (20).

### Identification of Treg-Related lncRNA Signature

To identify survival-related lncRNAs among Treg-related lncRNAs, we performed univariate Cox proportional hazard analysis (21). Treg-related lncRNAs in univariate analysis  $P < 0.01$  were included in the Least Absolute Shrinkage and Selection Operator (Lasso) regression. A multivariate Cox regression model was finally used to construct a prognostic signature based on the candidate Treg-related lncRNAs generated from the Lasso regression results (22–24).

### Construction and Application of Prognostic Model

A multivariate Cox regression model was used to establish an independent prognostic signature. The risk score for each patient sample was calculated as the expression value of each lncRNA multiplied by the sum of their weights in the multivariable Cox model. The median risk score was used to separate patients into

high- and low-risk groups. To validate the predictive value of the model, we performed the Kaplan–Meier log-rank test and time-dependent ROC curve analysis which were used to compare survival between high and low-risk groups in the training, testing, and total cohorts.

## Validation of Prognostic Signature

Univariate and multivariate Cox regression analyses were performed on the clinical data to determine whether the risk score is an independent indicator of prognosis. ROC curve analysis by univariate and multivariate Cox regression was performed to analyze the correlation between prognosis and clinicopathological factors including age, gender, tumor size (T), lymph node metastasis (N), distant metastasis (M), clinical stage, and risk score. Time-dependent receiver operating characteristic (ROC) curves were plotted to evaluate the accuracy of different clinicopathological factors and risk scores in predicting survival time by using the survival ROC R package (25). Finally, we constructed a prediction model by using nomogram. We then tested the accuracy of the prediction model through 3-year and 5-year calibration curves.

## Correlation Analysis of the 17 Treg-Related lncRNAs With Clinicopathological Factors

The expression of the 17 Treg-related lncRNAs were correlated with clinicopathological factors using the ggpubr R package. Moreover, we analyzed the correlation of 17 Treg-related lncRNAs the overall HNSCC patient survival.

## Analysis of Tumor Immune Microenvironment in High- and Low-Risk Patient Group

Principal component analysis (PCA) was used for effective dimensionality reduction, pattern recognition, and exploratory visualization of high-dimensional data of the whole-genome expression profiles retrieved from TCGA, 462 Treg-related coding genes, and 17-lncRNA signature expression profiles. Gene set enrichment analysis of (GSEA, <http://www.gsea-msigdb.org/gsea/index.jsp>) in high- and low-risk groups. GSEA was used for gene functional annotation and is a powerful analytical method for comparing genes with predefined gene sets obtained from whole genome expression profiles (26). In our experience, GSEA tends to have high repeatability and explanatory power in the analysis of molecular map data. Finally, gene expression matrix data were screened and analyzed by CIBERSORT (<https://cibersortx.stanford.edu/>) (27). Specifically, immune cell populations of infiltrating T cells in high- and low-risk groups were compared to access the relationship between 17-lncRNA signature and immune cell infiltration.

## RESULTS

### Identification of Treg-Related mRNA

The flowchart in **Figure 1** describes the order of computational steps we undertook to identify 17 lncRNAs. First, we obtained

18,392 mRNA and 9,357 lncRNA expression profiles which corresponded to clinical data from 453 patients registered in TCGA database. In the GSE15659 dataset from GEO, a total of 648 differentially expressed transcripts were obtained (**Table S1**). The data was divided into 281 up-regulated and 367 down-regulated transcripts and visualized using Volcano plot (**Figure 2A**). The top 50 differentially expressed transcripts were graphed as heat map using the heatmap R package (**Figure 2B**). 462 mRNA present in both GSE15659 and TCGA datasets were identified using Venn Software Analysis. The resulting overlapping mRNA were named Treg-related mRNAs for HNSCC (**Figure 2C**). Data enrichment was used to gather functional information (GO and KEGG) utilizing the Database for Annotation, visualization and integrated discovery (DAVID). Biological pathways related to Treg cell expression, included insulin secretion pathway (28, 29), pancreatic secretion pathway, Hippo signaling pathway (30–32) and others (**Figure S1A** and **Table S2**). In addition, the Treg-related mRNA transcripts related to microglial cell activation, cell adhesion and cell-cell communication were detected (**Figure S1B** and **Table S2**).

### Identification of 17-Treg-Related-lncRNA Signature for the Prognosis of Patients With HNSCC

The total cohort of 453 patients with HNSCC was randomly divided into training and testing cohorts at ratio of 1:1. In the training cohort, 1652 lncRNAs correlated with Treg-related mRNAs in patients with HNSCC (**Table S3**) and were designated as Treg-related lncRNAs. Following that, 35 lncRNAs were identified by Univariate Cox regression analysis (**Table S4**). Lasso regression analysis was carried out on 35 prognostic lncRNAs to improve confidence in the prediction. We identified 17 lncRNAs prognostic factors for patients with HNSCC (**Figures 3A, B**) (22). The correlation between Treg-related mRNAs and the associated lncRNAs is shown in **Figure S2** and **Table S5**. Of 17 assigned lncRNAs, additional multivariate Cox regression analysis of defined transcripts LINC00460 and AC092115.3 as significant independent prognostic factors (**Figure 3C**). These lncRNAs were then used to establish lncRNA prognostic signature. Six lncRNAs, namely, CAVIN2-AS1, AC007878.1, LINC00460, AC092115.3, AC068446.2, and LINC01976, were used to calculate risk factors for the prognosis of patients with HNSCC using the cutoff of HR>1. Meanwhile, 11 lncRNAs (AL157414.1, LINC01281, GLYCTK-AS1, LINC02325, AC026362.1, AL049552.1, STARD4-AS1, AC103809.1, AC104083.1, AC004461.2, and LINC02202) were protective factors for the prognosis of patients with HNSCC with the cutoff of HR<1 (**Figure 3C** and **Table S6**). The risk score for prognosis was calculated as Risk score =  $\sum_i \text{Expi}(\text{lncRNA}_i) * \text{Coef}(\text{lncRNA}_i)$  where Expi is the expression value of each lncRNA, and Coef is the regression coefficient of the multivariate Cox analysis for the target lncRNA (21, 23).

### Validation of the 17 -lncRNA Signature for HNSCC Prognosis

Median risk score for 17-lncRNA obtained in prognosis model was used to divide patients with HNSCC into high- and low-risk

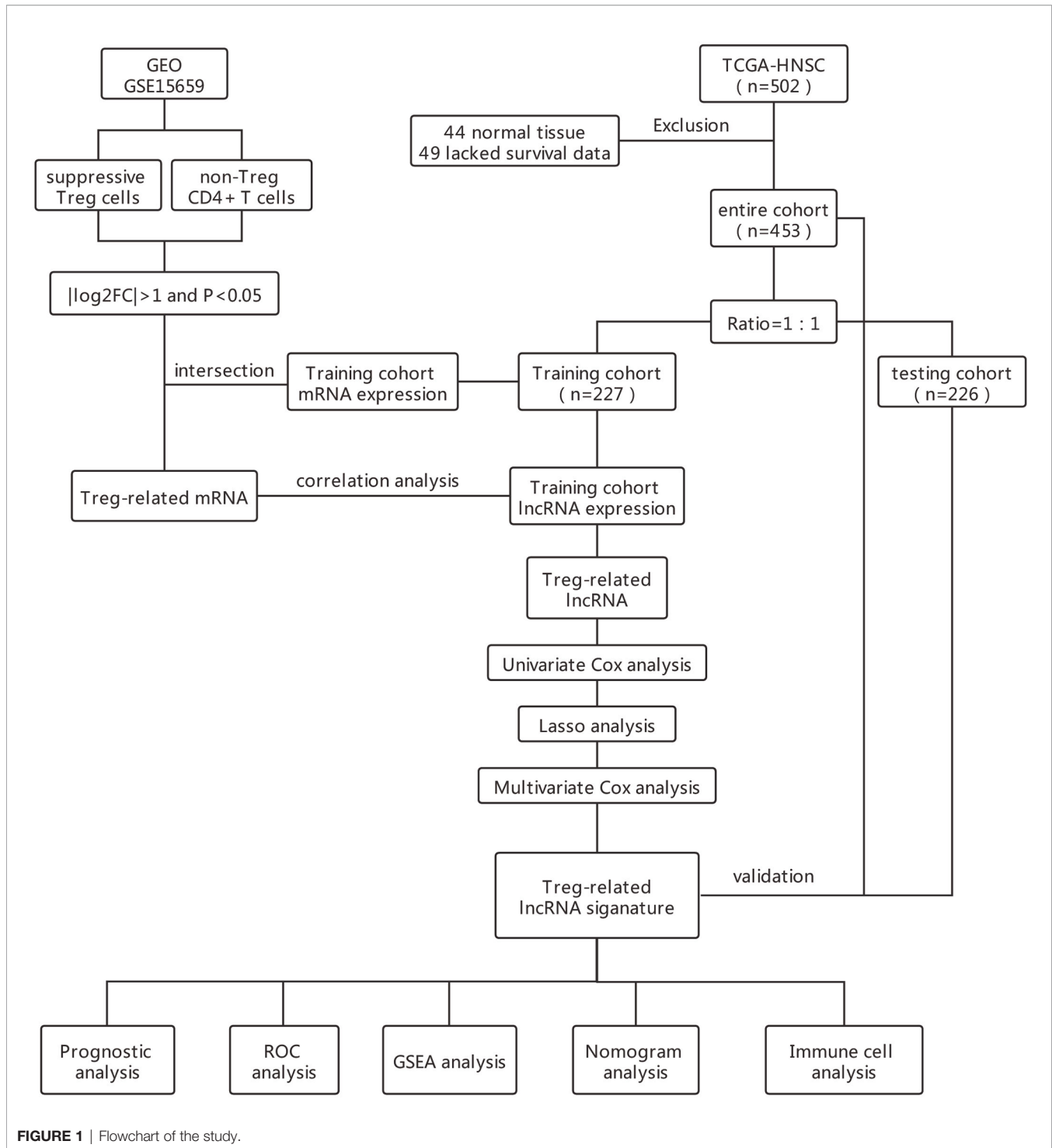
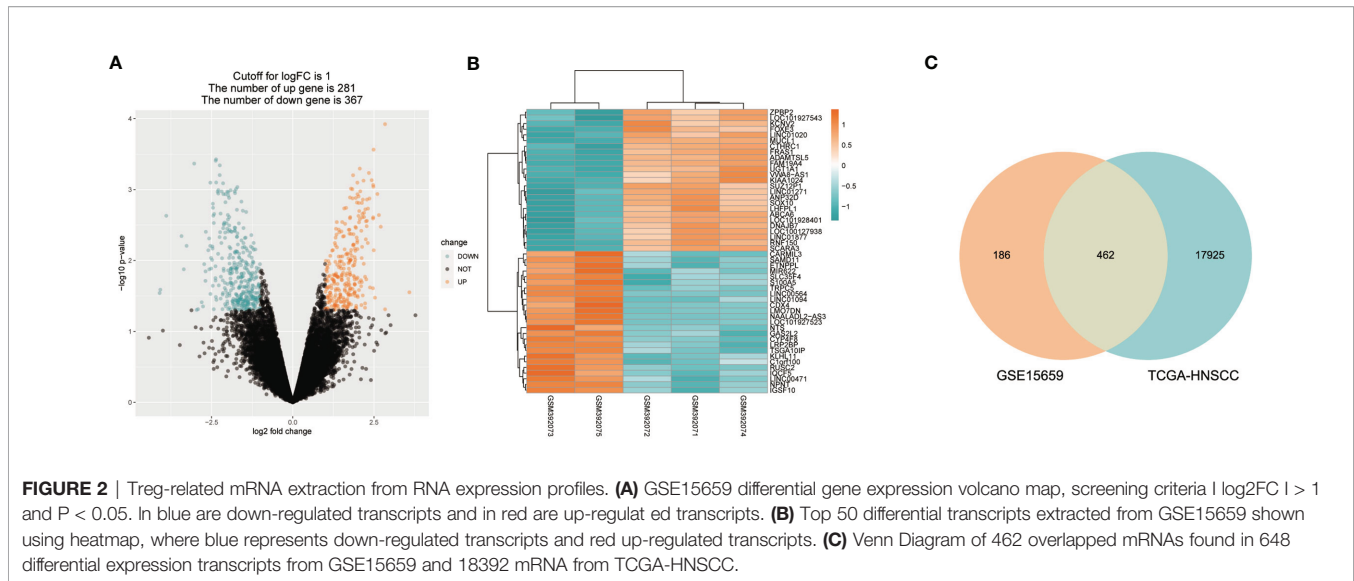


**FIGURE 1** | Flowchart of the study.

groups. We first used scatter plot (Figures 4A–C) and risk curve (Figures 4D–F) to describe the risk score and survival status of each patient with HNSCC, in the training, testing and total cohorts. The risk coefficient and mortality rate in the low-risk

group were lower than those in the high-risk group. The observed mortality rate correlated with the risk score (Figures 4A–F). The heatmap showed that CAVIN2-AS1, AC068446.2, LINC01976, AL157414.1, LINC00460, and



AC092115.3 were highly expressed in the high-risk group, while AC007878.1, LINC01281, GLYCTK-AS1, LINC02325, AC026362.1, AL049552.1, STARD4-AS1, AC103809.1, AC104083.1, AC004461.2, and LINC02202 were highly expressed in the low-risk group (Figures 4G–I). To assess further the accuracy of 17-lncRNA prognostic signature, we constructed the K-M survival curve using the R package “survival”. In the training cohort, the overall survival (OS) of the low-risk group was better than that of the high-risk group ( $P < 0.001$ , Figure 4J). These results in the testing cohort ( $P < 0.001$ , Figure 4K) and total cohort ( $P < 0.001$ , Figure 4L) were consistent with the results of the training cohort. The risk score correlated with the OS time of patients with HNSCC and hence is a good predictive value for HNSCC prognosis. To further evaluate model quality, we calculated area under the Curve (AUC) for the 3, 5 and 8-year survival curves using the time ROC R package. The AUC values were 0.829, 0.766, and 0.758 in the 3-, 5-, and 8-year follow-ups of the training cohort (Figure 4M) and 0.615, 0.578, and 0.58 in the testing cohort (Figure 4N). In the total cohort, the values were 0.721, 0.679, and 0.668, respectively (Figure 4O). Hence, the 17-lncRNA signature is a reliable measure of prognostic signature of HNSCC.

### Risk Score Is Independent Prognostic Factor for Patients With HNSCC

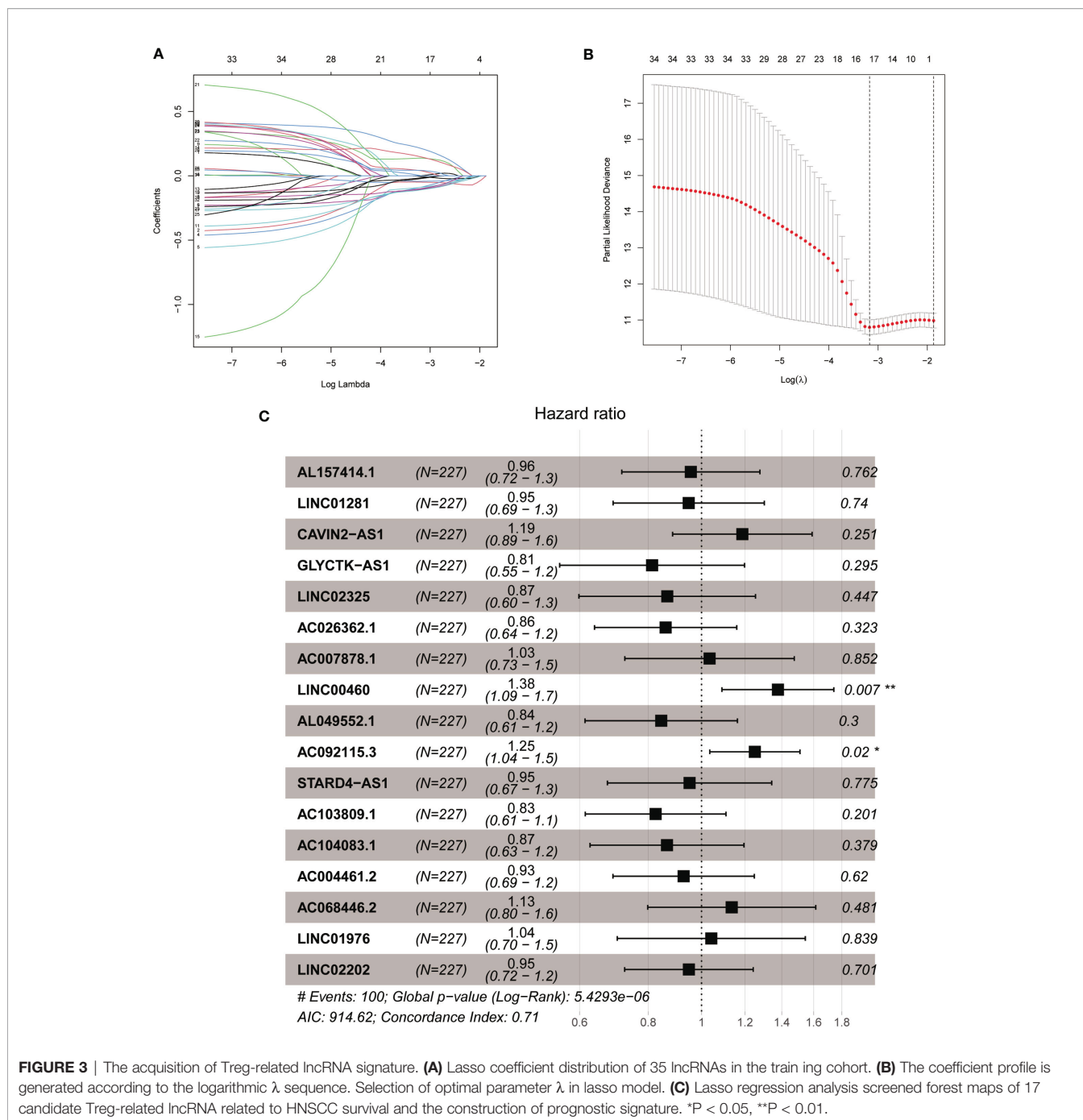
To further evaluate the risk score as an independent prognostic marker for patients with HNSCC, we performed univariate COX regression analysis comparing the risk score to other clinicopathological factors (age, gender, tumor size (T), lymph node metastasis (N), distant metastasis (M), clinical stage) using the survival ROC R package (Figures 5A–C). Age, gender, M, and risk score were independent prognostic indicators for patients with HNSCC. Through the multivariate COX regression analysis, we found that M and risk score were correlated with OS in the training cohort (Figure 5D). The multivariate COX regression analysis result of ‘M’ for OS showed

p values  $< 0.05$  in the training, testing (Figure 5E) and total cohorts (Figure 5F), indicating that M was a significantly independent prognostic factor for HNSCC. In the same way, ‘risk score’ was also a significantly independent prognostic factor for HNSCC in the training, testing, and total cohorts. The multivariate COX regression analysis suggested that the risk score containing 17-lncRNA signature was a significant prognostic factor for HNSCC, independent of clinicopathological parameters. The sensitivity and specificity of the risk score in predicting the prognosis of patients with HNSCC was investigated by comparing the area under the ROC curve (Figure 5G) which measured changes in the risk score and other clinicopathological factors in predicting the overall survival of HNSCC patients. The AUC values of the risk score, age and M were 0.693, 0.536, and 0.506, respectively. The risk score showed a better AUC than other clinicopathological factors, indicating that risk score is more effective in predicting HNSCC prognosis.

In attempt to develop a clinically applicable method for predicting the survival probability of patients, we generated a nomogram using the rms R package (Figure 5H), plotting risk score, age, and M. The risk score had the biggest contribution to the 3- and 5-year OS of patients with HNSCC. In addition, we supplemented our model with the 3-year and 5-year calibration charts. The 3- and 5-year OS calibration curves were well predicted compared with the ideal models in all cohorts (Figure 5I). The results showed that the nomogram can independently evaluate survival of patients with HNSCC, which may help doctors to make better medical decisions and follow-up plans.

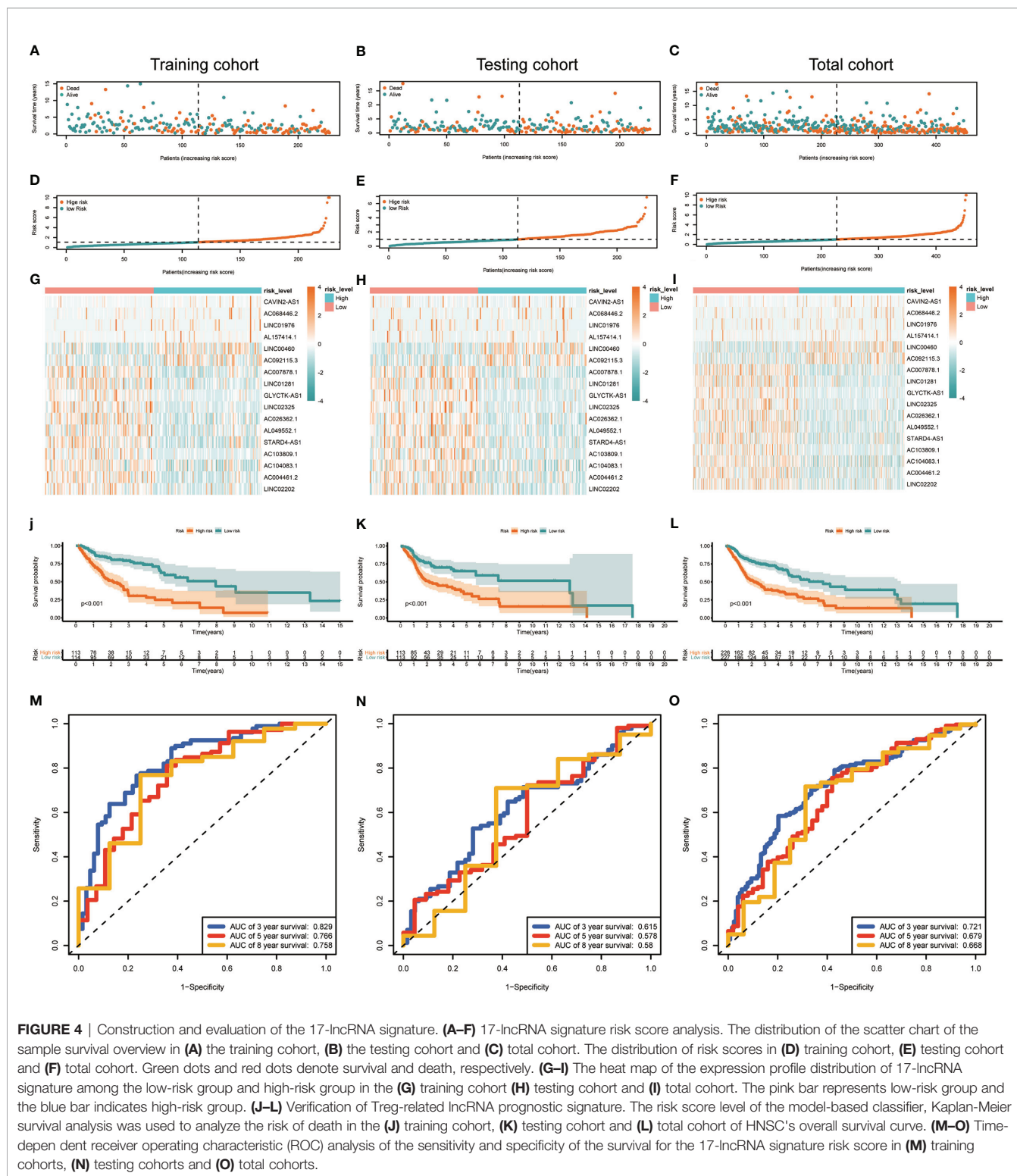
### Correlation of the Expression of the 17-lncRNA Signature With Clinicopathological Factors

The 17-lncRNA signature has been revealed effective for predicting HNSCC prognosis in aforementioned algorithm. However, whether each lncRNA has correlation with



clinicopathological factors still remains unclear and needs to be further assessed separately (**Figure S3**). Eleven lncRNAs were associated with disease progression, and included AL157414.1, LINC01281, CAVIN2-AS1, GLYCTK-AS1, LINC02325, AC026362.1, AC007878.1, LINC00460, AL049552.1, AC092115.3, STARD4-AS1, AC103809.1, AC104083.1, AC004461.2, AC068446.2, and LINC01976. Furthermore, three lncRNAs, namely, AC092115, GLYCTK-AS1, and LINC02202, were associated with different TNM classification of HNSCC. The expression of six lncRNAs such as LINC02325, AC026362.1,

AL049552.1, AC103809.1, LINC01976, and LINC02202 was statistically significant between different genders, while no statistically significant difference was observed for 17 lncRNAs among different age groups (**Figure S4**). Kaplan-Meier curves reveal that high expression of LINC00460, AC092115.3 and low expression of LINC01281, LINC02325, AC026362.1, AC007878.1, AL049552.1, STARD4-AS1, AC104083.1, AC004461.2 was associated with poor survival ( $P < 0.05$ ). Only ten of the 17 individual lncRNAs had a survival prediction power for HNSCC.



## Differences of Tumor Immune Microenvironment Between the Low- and High-Risk HNSCC Groups

Principal Component Analysis (PCA) was performed to evaluate expression differences among the low- and high-risk groups. Whole-

genome expression profiles from the TCGA and 462 Treg-related genes was insufficient to separated high and low risk groups (**Figures 6A, B**). However, the expression differences in 17-lncRNA signature could obviously distinguish high-risk patients from low-risk patients (**Figure 6C**). The GSEA analysis confirmed

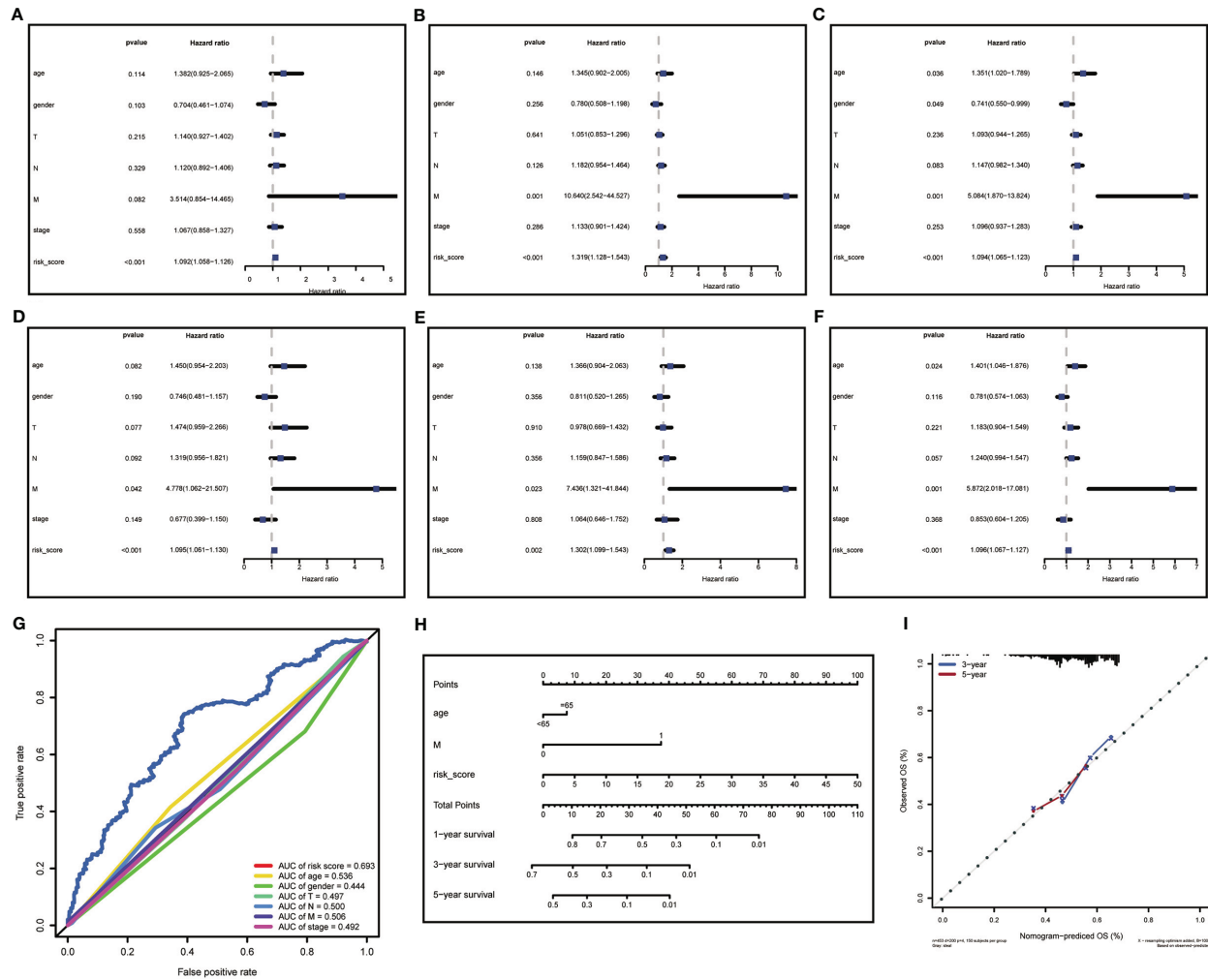


**FIGURE 5 |** Risk score analysis and nomogram construction to evaluate of overall survival in of HNSCC patients. **(A–C)** The independent prognostic value of risk score was evaluated by Cox regression analysis. Univariate Cox regression analysis of models in **(A)** training cohort, **(B)** testing cohort and **(C)** total cohort. **(D–F)** The independent prognostic value of risk score was evaluated by Cox regression analysis. Multivariate Cox regression analysis of models in **(D)** training cohort, **(E)** testing cohort and **(F)** total cohort. **(G)** ROC analysis of the ability of risk score and other clinicopathological factors to predict the overall survival of HNSCC. **(H)** Nomogram for predicting the overall survival rate of HNSCC. **(I)** Nomogram calibration chart during 3-year and 5-year follow-up.

that mRNAs related 17-lncRNA detected in the low-risk groups were enriched for transcripts related to immune-related biological processes- immune system development, leukocyte mediated immunity, and regulation of immune system process (Figures 6D–F). and in addition, the low-risk group had a better overall immune response than the high-risk group. The infiltrating immune cells in the HNSCC microenvironment were analyzed by CIBERSORT to explore the differences of immune cell infiltration between high-and low-risk group. Genes related to the naive B cells, CD8 T cells, memory activated CD4 T cells, follicular helper T cells, and regulatory T cells (Tregs) were found to be expressed at higher levels in low-risk group rather than in high-risk group (Figure 6G). In addition, expression of naive T cells, memory resting CD4 T cells, macrophage M0, and activated mast cells was significantly lower in low-risk group than in high-risk group (Figure 6G). These results

suggest that 17-lncRNA signature model is capable of distinguishing tumor microenvironment in the low and high-risk groups of HNSCC patient population.

## DISCUSSION

A subgroup of CD4+T cells, referred to as Treg cells can inhibit anti-tumor immune response and mediate tumor immune escape (33). Therapeutic targeting of Treg cells can effectively prolong the survival time of patients with tumors. Although Treg cell infiltration plays a central role in the pathogenesis of cancer, the heterogeneity of Treg cells paints a conflicting picture as to the ultimate effect of Tregs on cancer progression and patient prognosis. Suppressive Treg cells inhibit immune response



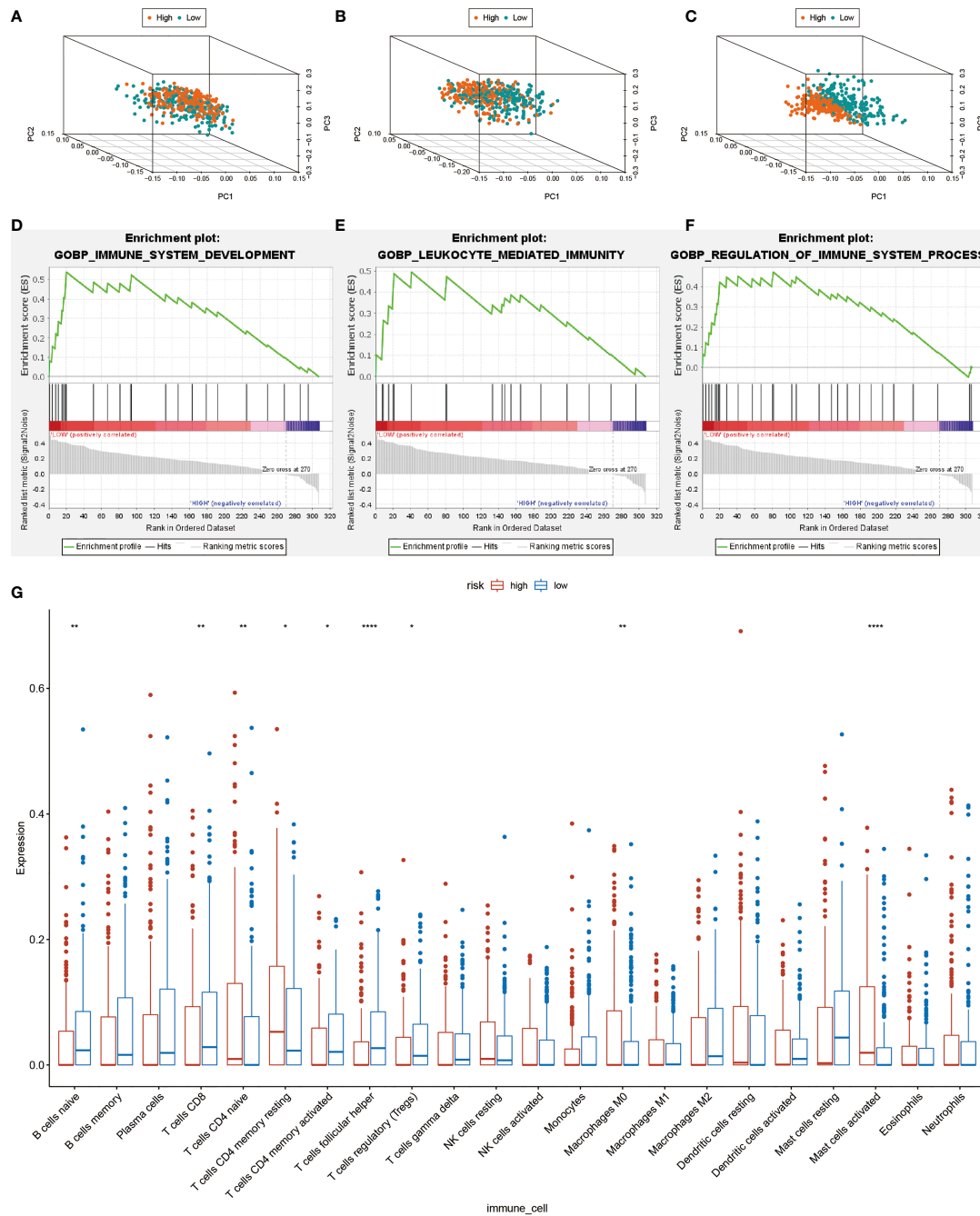


**FIGURE 6** | Computational analysis of immune cell infiltration in HNSCC patients. **(A)** All cohort PCA diagrams of genome-wide expression profiles of TCGA. **(B)** Cohort PCA diagrams of 462 Treg-related mRNA. **(C)** PCA diagram of all cohort of 17- lncRNA signature. **(D–F)** GSEA analysis. Results of functional enrichment of GSEA genes in different groups. **(G)** the difference in the expression of infiltrating immune cells between the high-risk group and the low-risk group. \* $P < 0.05$ , \*\* $P < 0.01$ , \*\*\* $P < 0.001$ , \*\*\*\* $P < 0.0001$ .

leading to immune escape of tumors (33). Activated Tregs, on the other hand, mediate tumor suppression by secreting immunosuppressive cytokines such as IL-10 (34). The resting Tregs, expressing lower levels of FoxP3, mediate suppression by secreting immunosuppressive cytokines such as TGF- $\beta$  and are less potent at suppressing proliferation and cytokine production

by effector T cells (7, 34). Non-suppressive Treg cells are known to secrete pro-inflammatory cytokines and their presence was correlated with tumor invasion by bacteria (7, 12). In the TME, lncRNAs regulate expression of molecules (e.g. PD-L1, MHC I, and HLA-G) on the surface of the tumor cells, which may help attenuate the function of effector T cell (35).

The goal of this study was to identify and validate lncRNA prognostic signature that gives rise to regulatory T cells, which can help provide a more individualized risk-assessment for HNSCC treatment. The prognostic value of 17-lncRNA was confirmed and validated by rigorous computational techniques including Kaplan-Meier analysis, ROC analyses, and multivariate Cox regression. We learned that the 17-lncRNA signature could accurately reflect the infiltration status of Treg cell, hence permitting identification of high-risk HNSCC patients with poor survival outcomes.

Among previously reported 17 lncRNAs, only LINC00460, LINC01281, STARD4-AS1, and LINC02202 were studied in HNSCC. Jiang (36) reported that LINC00460 could effectively induce epithelial-mesenchymal transition in Peroxiredoxin-1 dependent manner, enhancing the tumor cell proliferation and metastasis of HNSCC. LINC00460 was also shown to reduce stanniocalcin-2 by up-regulating microRNA-206 which triggers cellular autophagy, thereby affecting the progression of HNSCC (37). The molecular mechanism, by which LINC00460 influences the tumor microenvironment and regulates Treg cells remains unknown.

LINC01281 were reported to modulate the overall survival rate of patients with laryngeal squamous cell carcinoma by activating Wnt signaling pathway important for cellular proliferation, migration, and apoptosis (38). Our analysis also identifies LINC01281 as a potential biomarker for patients with HNSCC. Fourteen additional lncRNAs have not been previously reported to be potential prognostic targets for HNSCC. lncRNA AC092115.3 is a new novel signature that significantly associated with the prognosis of patients with HNSCC. We also found a high positive correlation between AC092115.3 and pirin (PIR), which can interact with oncoprotein B-cell lymphoma 3 code and nuclear factor I and participate in the activation of nuclear factor  $\kappa$ B (NF- $\kappa$ B) (39, 40). Classical NF- $\kappa$ B subunits p65 and c-Rel play a key role in the identity and function of Tregs (41, 42). Hence, AC092115.3 may affect the inhibitory effect of Treg cells on tumor immunity by regulating NF- $\kappa$ B transcriptional activity of specific target genes mediated by PIR.

Many additional differences in immune cell infiltration between high- and low-risk patients with HNSCC were discovered using 17-lncRNA signature model. For example, the infiltration levels with anti-tumor T cells like CD8 T cells, CD4 memory activated T cells, and follicular helper T cells were higher in the low-risk group compared to the high-risk group. Meanwhile, tumor-promoting cells like naive CD4+ T cells, macrophage Mo cells, and activated mast cells were detected in high-risk rather than low-risk group patients. These findings are consistent with the role CD8+T cells (43, 44) and systemic CD4+ T cells (45, 46) play in mediating durable antitumor responses (47). CD8+ T cells, especially IFN $\gamma$ + CD8+ T cells, are considered major drivers of anti-tumor immunity (48), and IFN $\gamma$  could enhance the activation of naive T cells in the tumor (43). The CD4+ T cells could eliminate tumor cells directly through cytolytic activity (49). Moreover, the activated CD4+ T cells are able to reshape the tumor immune microenvironment and facilitate tumor clearance (50). So, more infiltration with CD8 T and activated CD4 T cells and less activation of naive CD4 T cells is beneficial for HNSCC prognosis.

In addition, an obvious infiltration of activated mast cells (MCs) was observed in high-risk group. Infiltration with mast cells inside tumor microenvironment correlates with increased intratumoral microvessel density, enhancing tumor growth and tumor invasion, and inducing overall poor clinical outcome (51). Activated MCs promote IL-6 expression and decrease Th1/Th2 cytokines to skew Tregs towards IL-17-producing T cells (Th17) (52). These results suggested that reduced Treg cell recruitment with concomitant increase in Th17 infiltration may affect the poor prognosis (53, 54).

M0 macrophages accounted for a higher proportion of high-risk group, indicating that they may also play an immunosuppressive role inside tumor immune microenvironment (55). However, we didn't observe statistically significant differences of M1 and M2 macrophage populations between low- and high-risk groups. Since the infiltration counts of M1 and M2 macrophages were unknown, we predict that tumor-associated macrophage polarization (M1/M2 ratio) was another potential indicator of patient prognosis (56, 57). The overall level of Treg cell infiltration was significantly higher in the low-risk group than high-risk group.

It is generally accepted that Treg cells help promote tumor immune escape, however more recent studies suggest that Tregs are heterogeneous in nature with different Treg populations having opposite effect on tumor microenvironment (7). Two types of Treg cells were identified including suppressive resting and activated Tregs, and nonsuppressive Treg (7). In addition, studies have suggested that infiltrating and circulating Treg cells may lead to different prognostic outcomes in tumors (58, 59). Taken together, quantitative understanding of how to alter microenvironment of HNSCC will come from quantifying the ratios of suppressive to nonsuppressive Treg populations. Our results confirmed that tumor immune microenvironment in the low-risk group was more beneficial for tumor killing. We therefore suggest that 17-lncRNA signature is a good measure of tumor immune microenvironment, and thus a good predictor of HNSCC prognosis.

Our study integrated bioinformatics analysis with the knowledge of tumor immune microenvironment to identify and validate the 17-lncRNA signature for HNSCC prognosis, providing a new approach for further stratification among HNSCC patients. Future studies should attempt to clarify the mechanisms of how 17 Treg-related lncRNAs regulates tumor immune microenvironment in HNSCC, and provide new targets for HNSCC immunotherapy in the future.

## DATA AVAILABILITY STATEMENT

The datasets presented in this study can be found in online repositories. The names of the repository/repositories and accession number(s) can be found in the article/**Supplementary Material**.

## AUTHOR CONTRIBUTIONS

XS designed and directed the study. QS and YL organized the public data and wrote the manuscript. QS, XY, and XW

performed experimental work and analyzed the data. QS, YL, and ZL took charge for data visualization. XS, YL, and YM revised the manuscript. All authors contributed to the article and approved the submitted version.

## FUNDING

This work was supported by the Taishan Scholars Project (No. ts20190991) and the Natural Science Foundation of Shandong Province (No.: ZR2019PH113).

## REFERENCES

- Bray F, Ferlay J, Soerjomataram I, Siegel RL, Torre LA, Jemal A. Global Cancer Statistics 2018: GLOBOCAN Estimates of Incidence and Mortality Worldwide for 36 Cancers in 185 Countries. *CA Cancer J Clin* (2018) 68:394–424. doi: 10.3322/caac.21492
- Knopf A, Bahadori L, Fritsche K, Piontek G, Becker CC, Knolle P, et al. Primary Tumor-Associated Expression of CXCR4 Predicts Formation of Local and Systemic Recurrence in Head and Neck Squamous Cell Carcinoma. *Oncotarget* (2017) 8:112739–47. doi: 10.18632/oncotarget.22562
- Chow LQM. Head and Neck Cancer. *N Engl J Med* (2020) 382:60–72. doi: 10.1056/NEJMra1715715
- Zou W. Regulatory T Cells, Tumour Immunity and Immunotherapy. *Nat Rev Immunol* (2006) 6:295–307. doi: 10.1038/nri1806
- Shitara K, Nishikawa H. Regulatory T Cells: A Potential Target in Cancer Immunotherapy. *Ann N Y Acad Sci* (2018) 1417:104–15. doi: 10.1111/nyas.13625
- Khazaie K, von Boehmer H. The Impact of CD4+CD25+ Treg on Tumor Specific CD8+ T Cell Cytotoxicity and Cancer. *Semin Cancer Biol* (2006) 16:124–36. doi: 10.1016/j.semcancer.2005.11.006
- Miyara M, Yoshioka Y, Kitoh A, Shima T, Wing K, Niwa A, et al. Functional Delineation and Differentiation Dynamics of Human CD4+ T Cells Expressing the FoxP3 Transcription Factor. *Immunity* (2009) 30:899–911. doi: 10.1016/j.immuni.2009.03.019
- Taylor NA, Vick SC, Iglesia MD, Brickey WJ, Midkiff BR, McKinnon KP, et al. Treg Depletion Potentiates Checkpoint Inhibition in Claudin-Low Breast Cancer. *J Clin Invest* (2017) 127:3472–83. doi: 10.1172/jci90499
- Ganesan AP, Johansson M, Ruffell B, Yagui-Beltrán A, Lau J, Jablons DM, et al. Tumor-Infiltrating Regulatory T Cells Inhibit Endogenous Cytotoxic T Cell Responses to Lung Adenocarcinoma. *J Immunol* (2013) 191:2009–17. doi: 10.4049/jimmunol.1301317
- Smyth MJ, Teng MW, Swann J, Kyriakopoulos K, Godfrey DI, Hayakawa Y. CD4+CD25+ T Regulatory Cells Suppress NK Cell-Mediated Immunotherapy of Cancer. *J Immunol* (2006) 176:1582–7. doi: 10.4049/jimmunol.176.3.1582
- Zhuo C, Li Z, Xu Y, Wang Y, Li Q, Peng J, et al. Higher FOXP3-TSDR Demethylation Rates in Adjacent Normal Tissues in Patients With Colon Cancer Were Associated With Worse Survival. *Mol Cancer* (2014) 13:153. doi: 10.1186/1476-4598-13-153
- Saito T, Nishikawa H, Wada H, Nagano Y, Sugiyama D, Atarashi K, et al. Two FOXP3(+)/CD4(+) T Cell Subpopulations Distinctly Control the Prognosis of Colorectal Cancers. *Nat Med* (2016) 22:679–84. doi: 10.1038/nm.4086
- Salama P, Phillips M, Grieff F, Morris M, Zeps N, Joseph D, et al. Tumor-Infiltrating FOXP3+ T Regulatory Cells Show Strong Prognostic Significance in Colorectal Cancer. *J Clin Oncol* (2009) 27:186–92. doi: 10.1200/jco.2008.18.7229
- Jiang R, Tang J, Chen Y, Deng L, Ji J, Xie Y, et al. The Long Noncoding RNA lnc-EGFR Stimulates T-Regulatory Cells Differentiation Thus Promoting Hepatocellular Carcinoma Immune Evasion. *Nat Commun* (2017) 8:15129. doi: 10.1038/ncomms15129
- Sun CC, Zhu W, Li SJ, Hu W, Zhang J, Zhuo Y, et al. FOXC1-Mediated LINC00301 Facilitates Tumor Progression and Triggers an Immune-Suppressing Microenvironment in non-Small Cell Lung Cancer by Regulating the HIF1 $\alpha$  Pathway. *Genome Med* (2020) 12:77. doi: 10.1186/s13073-020-00773-y
- Ma W, Zhao F, Yu X, Guan S, Suo H, Tao Z, et al. Immune-Related lncRNAs as Predictors of Survival in Breast Cancer: A Prognostic Signature. *J Transl Med* (2020) 18:442. doi: 10.1186/s12967-020-02522-6
- Jin D, Song Y, Chen Y, Zhang P. Identification of a Seven-lncRNA Immune Risk Signature and Construction of a Predictive Nomogram for Lung Adenocarcinoma. *BioMed Res Int* (2020) 2020:7929132. doi: 10.1155/2020/7929132
- Wu ZH, Tang Y, Zhou Y. Alternative Splicing Events Implicated in Carcinogenesis and Prognosis of Thyroid Gland Cancer. *Sci Rep* (2021) 11:4841. doi: 10.1038/s41598-021-84403-6
- Li W, Liu J, Zhao H. Identification of a Nomogram Based on Long non-Coding RNA to Improve Prognosis Prediction of Esophageal Squamous Cell Carcinoma. *Aging (Albany NY)* (2020) 12:1512–26. doi: 10.18632/aging.102697
- Li X, Li Y, Yu X, Jin F. Identification and Validation of Stemness-Related lncRNA Prognostic Signature for Breast Cancer. *J Transl Med* (2020) 18:331. doi: 10.1186/s12967-020-02497-4
- Shen Y, Peng X, Shen C. Identification and Validation of Immune-Related lncRNA Prognostic Signature for Breast Cancer. *Genomics* (2020) 112:2640–6. doi: 10.1016/j.ygeno.2020.02.015
- Fan T, Pan S, Yang S, Hao B, Zhang L, Li D, et al. Clinical Significance and Immunologic Landscape of a Five-IL(R)-Based Signature in Lung Adenocarcinoma. *Front Immunol* (2021) 12:693062. doi: 10.3389/fimmu.2021.693062
- Fu D, Zhang B, Wu S, Zhang Y, Xie J, Ning W, et al. Prognosis and Characterization of Immune Microenvironment in Acute Myeloid Leukemia Through Identification of an Autophagy-Related Signature. *Front Immunol* (2021) 12:695865. doi: 10.3389/fimmu.2021.695865
- Li Z, Li Y, Wang X, Yang Q. Identification of a Six-Immune-Related Long Non-Coding RNA Signature for Predicting Survival and Immune Infiltrating Status in Breast Cancer. *Front Genet* (2020) 11:680. doi: 10.3389/fgene.2020.00680
- Kamarudin AN, Cox T, Kolamunnage-Dona R. Time-Dependent ROC Curve Analysis in Medical Research: Current Methods and Applications. *BMC Med Res Methodol* (2017) 17:53. doi: 10.1186/s12874-017-0332-6
- Subramanian A, Tamayo P, Mootha VK, Mukherjee S, Ebert BL, Gillette MA, et al. Gene Set Enrichment Analysis: A Knowledge-Based Approach for Interpreting Genome-Wide Expression Profiles. *Proc Natl Acad Sci U S A* (2005) 102:15545–50. doi: 10.1073/pnas.0506580102
- Newman AM, Liu CL, Green MR, Gentles AJ, Feng W, Xu Y, et al. Robust Enumeration of Cell Subsets From Tissue Expression Profiles. *Nat Methods* (2015) 12:453–7. doi: 10.1038/nmeth.3337
- Syed I, Rubin de Celis MF, Mohan JF, Moraes-Vieira PM, Vijayakumar A, Nelson AT, et al. PAHSAs Attenuate Immune Responses and Promote  $\beta$  Cell Survival in Autoimmune Diabetic Mice. *J Clin Invest* (2019) 129:3717–31. doi: 10.1172/jci122445
- Rigby MR, Harris KM, Pinckney A, DiMeglio LA, Rendell MS, Felner EI, et al. Alefacept Provides Sustained Clinical and Immunological Effects in New-Onset Type 1 Diabetes Patients. *J Clin Invest* (2015) 125:3285–96. doi: 10.1172/jci81722
- Ni X, Tao J, Barbi J, Chen Q, Park BV, Li Z, et al. YAP Is Essential for Treg-Mediated Suppression of Antitumor Immunity. *Cancer Discovery* (2018) 8:1026–43. doi: 10.1158/2159-8290.Cd-17-1124

## ACKNOWLEDGMENTS

This is a short text to acknowledge the contributions of specific colleagues, institutions, or agencies that aided the efforts of the authors.

## SUPPLEMENTARY MATERIAL

The Supplementary Material for this article can be found online at: <https://www.frontiersin.org/articles/10.3389/fimmu.2021.782216/full#supplementary-material>

31. Shi H, Liu C, Tan H, Li Y, Nguyen TM, Dhungana Y, et al. Hippo Kinases Mst1 and Mst2 Sense and Amplify IL-2r-STAT5 Signaling in Regulatory T Cells to Establish Stable Regulatory Activity. *Immunity* (2018) 49:899–914.e6. doi: 10.1016/j.immuni.2018.10.010
32. Harb H, Stephen-Victor E, Crestani E, Benamar M, Massoud A, Cui Y, et al. A Regulatory T Cell Notch4-GDF15 Axis Licenses Tissue Inflammation in Asthma. *Nat Immunol* (2020) 21:1359–70. doi: 10.1038/s41590-020-0777-3
33. Zhou W, Deng J, Chen Q, Li R, Xu X, Guan Y, et al. Expression of CD4+CD25+CD127(Low) Regulatory T Cells and Cytokines in Peripheral Blood of Patients With Primary Liver Carcinoma. *Int J Med Sci* (2020) 17:712–9. doi: 10.7150/ijms.44088
34. Zhan Y, Zhang Y, Gray D, Carrington EM, Bouillet P, Ko HJ, et al. Defects in the Bcl-2-Regulated Apoptotic Pathway Lead to Preferential Increase of CD25 Low Foxp3+ Anergic CD4+ T Cells. *J Immunol* (2011) 187:1566–77. doi: 10.4049/jimmunol.1100027
35. Luo Y, Yang J, Yu J, Liu X, Yu C, Hu J, et al. Long Non-Coding RNAs: Emerging Roles in the Immunosuppressive Tumor Microenvironment. *Front Oncol* (2020) 10:48. doi: 10.3389/fonc.2020.00048
36. Jiang Y, Cao W, Wu K, Qin X, Wang X, Li Y, et al. LncRNA LINC00460 Promotes EMT in Head and Neck Squamous Cell Carcinoma by Facilitating Peroxiredoxin-1 Into the Nucleus. *J Exp Clin Cancer Res* (2019) 38:365. doi: 10.1186/s13046-019-1364-z
37. Xue K, Li J, Nan S, Zhao X, Xu C. Downregulation of LINC00460 Decreases STC2 and Promotes Autophagy of Head and Neck Squamous Cell Carcinoma by Up-Regulating microRNA-206. *Life Sci* (2019) 231:116459. doi: 10.1016/j.lfs.2019.05.015
38. Zhang G, Fan E, Zhong Q, Feng G, Shuai Y, Wu M, et al. Identification and Potential Mechanisms of a 4-lncRNA Signature That Predicts Prognosis in Patients With Laryngeal Cancer. *Hum Genomics* (2019) 13:36. doi: 10.1186/s40246-019-0230-6
39. Liu F, Rehmani I, Esaki S, Fu R, Chen L, de Serrano V, et al. Pirin is an Iron-Dependent Redox Regulator of NF- $\kappa$ B. *Proc Natl Acad Sci U S A* (2013) 110:9722–7. doi: 10.1073/pnas.1221743110
40. Rius-Pérez S, Pérez S, Martí-Andrés P, Monsalve M, Sastre J. Nuclear Factor Kappa B Signaling Complexes in Acute Inflammation. *Antioxid Redox Signal* (2020) 33:145–65. doi: 10.1089/ars.2019.7975
41. Grinberg-Bleyer Y, Oh H, Desrichard A, Bhatt DM, Caron R, Chan TA, et al. NF- $\kappa$ B C-Rel Is Crucial for the Regulatory T Cell Immune Checkpoint in Cancer. *Cell* (2017) 170:1096–108.e13. doi: 10.1016/j.cell.2017.08.004
42. Oh H, Grinberg-Bleyer Y, Liao W, Maloney D, Wang P, Wu Z, et al. An NF- $\kappa$ B Transcription-Factor-Dependent Lineage-Specific Transcriptional Program Promotes Regulatory T Cell Identity and Function. *Immunity* (2017) 47:450–65.e5. doi: 10.1016/j.immuni.2017.08.010
43. St Paul M, Ohashi PS. The Roles of CD8(+) T Cell Subsets in Antitumor Immunity. *Trends Cell Biol* (2020) 30:695–704. doi: 10.1016/j.tcb.2020.06.003
44. Nikolova M, Lelievre JD, Carriere M, Bensussan A, Lévy Y. Regulatory T Cells Differentially Modulate the Maturation and Apoptosis of Human CD8+ T-Cell Subsets. *Blood* (2009) 113:4556–65. doi: 10.1182/blood-2008-04-151407
45. Oh DY, Kwek SS, Raju SS, Li T, McCarthy E, Chow E, et al. Intratumoral CD4(+) T Cells Mediate Anti-Tumor Cytotoxicity in Human Bladder Cancer. *Cell* (2020) 181:1612–25.e13. doi: 10.1016/j.cell.2020.05.017
46. Nelson MH, Knochelmann HM, Bailey SR, Huff LW, Bowers JS, Majchrzak-Kuligowska K, et al. Identification of Human CD4(+) T Cell Populations With Distinct Antitumor Activity. *Sci Adv* (2020) 6(27):eaba7443. doi: 10.1126/sciadv.aba7443
47. Sukumar M, Liu J, Mehta GU, Patel SJ, Roychoudhuri R, Crompton JG, et al. Mitochondrial Membrane Potential Identifies Cells With Enhanced Stemness for Cellular Therapy. *Cell Metab* (2016) 23:63–76. doi: 10.1016/j.cmet.2015.11.002
48. van der Leun AM, Thommen DS, Schumacher TN. CD8(+) T Cell States in Human Cancer: Insights From Single-Cell Analysis. *Nat Rev Cancer* (2020) 20:218–32. doi: 10.1038/s41568-019-0235-4
49. Borst J, Ahrends T, Båbala N, Melief CJM, Kastenmüller W. CD4(+) T Cell Help in Cancer Immunology and Immunotherapy. *Nat Rev Immunol* (2018) 18:635–47. doi: 10.1038/s41577-018-0044-0
50. Mandal R, Chan TA. Personalized Oncology Meets Immunology: The Path Toward Precision Immunotherapy. *Cancer Discov* (2016) 6:703–13. doi: 10.1158/2159-8290.Cd-16-0146
51. Watermann C, Pasternack H, Idel C, Ribbat-Idel J, Brägelmann J, Kuppler P, et al. Recurrent HNSCC Harbor an Immunosuppressive Tumor Immune Microenvironment Suggesting Successful Tumor Immune Evasion. *Clin Cancer Res* (2021) 27:632–44. doi: 10.1158/1078-0432.Ccr-20-0197
52. Piconese S, Gri G, Tripodo C, Musio S, Gorzaneli A, Frossi B, et al. Mast Cells Counteract Regulatory T-Cell Suppression Through Interleukin-6 and OX40/OX40L Axis Toward Th17-Cell Differentiation. *Blood* (2009) 114:2639–48. doi: 10.1182/blood-2009-05-220004
53. Punt S, Dronkers EA, Welters MJ, Goedemans R, Koljenović S, Bloemena E, et al. A Beneficial Tumor Microenvironment in Oropharyngeal Squamous Cell Carcinoma is Characterized by a High T Cell and Low IL-17(+) Cell Frequency. *Cancer Immunol Immunother* (2016) 65:393–403. doi: 10.1007/s00262-016-1805-x
54. Limagne E, Euvrard R, Thibaudin M, Rébéc C, Derangère V, Chevriaux A, et al. Accumulation of MDSC and Th17 Cells in Patients With Metastatic Colorectal Cancer Predicts the Efficacy of a FOLFOX-Bevacizumab Drug Treatment Regimen. *Cancer Res* (2016) 76:5241–52. doi: 10.1158/0008-5472.Can-15-3164
55. DeNardo DG, Ruffell B. Macrophages as Regulators of Tumour Immunity and Immunotherapy. *Nat Rev Immunol* (2019) 19:369–82. doi: 10.1038/s41577-019-0127-6
56. Mateu-Jimenez M, Curull V, Pijuan L, Sánchez-Font A, Rivera-Ramos H, Rodríguez-Fuster A, et al. Systemic and Tumor Th1 and Th2 Inflammatory Profile and Macrophages in Lung Cancer: Influence of Underlying Chronic Respiratory Disease. *J Thorac Oncol* (2017) 12:235–48. doi: 10.1016/j.jtho.2016.09.137
57. Hubert P, Roncarati P, Demoulin S, Pilard C, Ancion M, Reynders C, et al. Extracellular HMGB1 Blockade Inhibits Tumor Growth Through Profoundly Remodeling Immune Microenvironment and Enhances Checkpoint Inhibitor-Based Immunotherapy. *J Immunother Cancer* (2021) 9(3):ea00196. doi: 10.1136/jitc-2020-001966
58. Pacella I, Piconese S. Immunometabolic Checkpoints of Treg Dynamics: Adaptation to Microenvironmental Opportunities and Challenges. *Front Immunol* (2019) 10:1889. doi: 10.3389/fimmu.2019.01889
59. Takasato Y, Kurashima Y, Kiuchi M, Hirahara K, Murasaki S, Arai F, et al. Orally Desensitized Mast Cells Form a Regulatory Network With Treg Cells for the Control of Food Allergy. *Mucosal Immunol* (2021) 14:640–51. doi: 10.1038/s41385-020-00358-3

**Conflict of Interest:** The authors declare that the research was conducted in the absence of any commercial or financial relationships that could be construed as a potential conflict of interest.

**Publisher's Note:** All claims expressed in this article are solely those of the authors and do not necessarily represent those of their affiliated organizations, or those of the publisher, the editors and the reviewers. Any product that may be evaluated in this article, or claim that may be made by its manufacturer, is not guaranteed or endorsed by the publisher.

Copyright © 2021 Sun, Li, Yang, Wu, Liu, Mou and Song. This is an open-access article distributed under the terms of the Creative Commons Attribution License (CC BY). The use, distribution or reproduction in other forums is permitted, provided the original author(s) and the copyright owner(s) are credited and that the original publication in this journal is cited, in accordance with accepted academic practice. No use, distribution or reproduction is permitted which does not comply with these terms.